

# Intrinsic Enantioselectivity of Natural Polynucleotides Modulated by Copper Ions

YAN FU, XIONGFEI CHEN, JINLI ZHANG, AND WEI LI\*

Key Laboratory of Systems Bioengineering MOE, Key Laboratory for Green Chemical Technology MOE, Tianjin University; Collaborative Innovation Center of Chemical Science and Chemical Engineering, Tianjin, People's Republic of China

**ABSTRACT** Natural polynucleotides including *Micrococcus lysodeikticus* and calf thymus DNA exhibit enantioselective recognition to S-ofloxacin regulated by Cu<sup>2+</sup>. This is the first report that ofloxacin and Cu<sup>2+</sup> have cooperative effects on the local distortions of polynucleotides. At the [Cu<sup>2+</sup>]/[base] ratio of 0.1, S-ofloxacin is more liable to induce the locally distorted structures of polynucleotides, of which the association constant of S-ofloxacin toward DNA-Cu(II) is three times higher than that of the R-enantiomer. The apparent increase of adsorption capability and cooperativity, as well as the change of adsorption mechanism were detected in the adsorption of ofloxacin enantiomers on polynucleotides upon Cu(II)-coordination. This study not only discloses the effect of the chiral drug on the structural transition of long double-stranded DNA, but provides fundamental data to develop a novel enantioseparation method based on natural polynucleotides. *Chirality* 27:306–313, 2015. © 2015 Wiley Periodicals, Inc.

**KEY WORDS:** chirality; DNA; ofloxacin; enantioseparation; copper; adsorption

Natural polynucleotides, one of the abundant multifunctional biomacromolecules, have been widely used to explore helical architectures, asymmetric catalysts, and chiral selectors, due to the intrinsic chirality, well-defined structure, and specific molecular recognition of DNA.<sup>1–4</sup> Compared with oligonucleotides, polynucleotides possess several intriguing features in the enantioselective resolution. First, positive cooperativity exists in the stereoselective interactions between daunorubicin enantiomers and [poly(dGdC)]<sub>2</sub>.<sup>5</sup> Second, polynucleotides consisting of more than 1 kbp are susceptible to undergo single-molecule compaction. In the folding transition process, a long DNA strand showed chiral discrimination ability.<sup>6,7</sup> Zhang et al. reported that oxaliplatin and its enantiomer exhibited a distinct mechanism in the condensation process of λ-DNA. The di-adduct formation rate of Pt(R,R-DACH) was higher than that of Pt(S,S-DACH); however, the proportions of micro-loops and long-range crosslinks for Pt(S,S-DACH) were higher than those for Pt(R,R-DACH).<sup>8</sup> Third, polynucleotides exhibit a high feasibility in the enantioseparation through ultrafiltration or dialysis method. For example, salmon testes DNA was immobilized onto the chitosan membrane via the Pt(II)-associated coordination, and such a DNA-immobilized chitosan membrane showed a preferential enrichment of D-phenylalanine with a separation factor about 1.5.<sup>9</sup> In order to explore the substantial application of chiral selectors based on polynucleotides, it is fundamental to study efficient methods to enhance the enantioselectivity and adsorption capacity of polynucleotides towards different enantiomers.

Ofloxacin (as illustrated in Fig. 1), a member of the quinolone antibiotics, which exhibits antibacterial activity by inhibiting the action of Type II topoisomerase, was originally proposed to bind to DNA molecules.<sup>10–13</sup> Previous studies have shown that the enantioselective discrimination of short duplexes (10–22 bp) toward S-ofloxacin against R-ofloxacin was attributed to the steric hindrance between the methyl group of ofloxacin and the phosphate backbone of DNA. Interestingly, a distinct discrimination mechanism was involved in the enantioselective recognition of ofloxacin enantiomers between

GC- and AT-rich oligonucleotides.<sup>14–16</sup> For example, ofloxacin partially intercalated into DNA base pairs from the minor groove of the GC-rich duplex, and Cu<sup>2+</sup> acted as a bridge to connect the N7 and/or O6 sites of guanines with the carboxylic and the carbonyl groups of ofloxacin. In contrast, for the AT-rich sequence, ofloxacin interacted with Cu(II) through the groove binding model without intercalation. To overcome the intrinsic limitations of natural polynucleotides, herein we were motivated to investigate a method to enhance the enantioselectivity and the adsorption capacity of long double-stranded DNA molecules from *Micrococcus lysodeikticus* and calf thymus, characterized by using circular dichroism (CD), fluorescence spectroscopy, dynamic light scattering (DLS), UV melting analysis, atomic force microscopy (AFM), and high-performance liquid chromatography (HPLC). It is known that these natural polynucleotides exhibit enantioselective recognition toward S-ofloxacin regulated by Cu<sup>2+</sup>. Interestingly, ofloxacin and Cu<sup>2+</sup> have cooperative effects on the local distortions of polynucleotides. The apparent increase of binding affinity and binding cooperativity, as well as the change of adsorption mechanism, are detected between ofloxacin enantiomers and polynucleotides upon Cu(II)-coordination.

## MATERIALS AND METHODS

### Materials

*Micrococcus lysodeikticus* DNA (denoted ML DNA, GC% = 72) and calf thymus DNA (denoted CT DNA, GC% = 42) were purchased from Sigma-Aldrich (St. Louis, MO). DNA concentrations in aqueous solution were determined by measuring the UV adsorption at 260 nm. The

Contract grant sponsor: NSFC; Contract grant number: 21206107.

Contract grant sponsor: National High-tech R&D Program of China; Contract grant number: 2012AA03A609.

\*Correspondence to: Wei Li, Key Laboratory of Systems Bioengineering MOE, Key Laboratory for Green Chemical Technology MOE, Tianjin University; Collaborative Innovation Center of Chemical Science and Chemical Engineering (Tianjin), 92 Weijin Road, Nankai District, Tianjin 300072, P.R. China. E-mail: liwei@tju.edu.cn

Received for publication 13 November 2014; Accepted 7 January 2015

DOI: 10.1002/chir.22430

Published online 09 February 2015 in Wiley Online Library (wileyonlinelibrary.com).

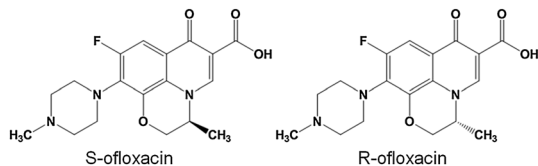


Fig. 1. Chemical structures of *S*- and *R*-ofloxacin.

average extinction coefficients were  $6600 \text{ M}^{-1}\cdot\text{cm}^{-1}$  for CT DNA and  $6840 \text{ M}^{-1}\cdot\text{cm}^{-1}$  for ML DNA (expressed as DNA bases). Racemic and *S*-ofloxacin were purchased from Jianglai Biological Technology (China), with a purity higher than 98.0%. *R*-ofloxacin was provided by Daicel Chiral Technologies (Tokyo, Japan), with a purity higher than 98.0%.  $\text{CuCl}_2\cdot 2\text{H}_2\text{O}$  was purchased from Alfa Aesar (Ward Hill, MA). Methyl green (MG) and ethidium bromide (EB) were purchased from Sigma-Aldrich. Ultrafiltration centrifugal tubes (Nanosep 3K, Omega), were purchased from Pall (East Hills, NY).

### CD Spectroscopy

CD experiments were carried out using Jasco J-810 spectropolarimeter equipped with a Julabo temperature controller. For titration experiments, samples of  $800 \mu\text{M}$  DNA (calculated from base concentration) were titrated with different concentration of  $\text{Cu}^{2+}$ . CD spectra were recorded from 350 nm to 190 nm at  $25^\circ\text{C}$  using a quartz cuvette of 0.1 cm path length with a scanning speed of 100 nm/min.

For competitive binding assays, DNA-Cu(II)-MG was prepared as follows: concentrated  $\text{CuCl}_2$  solution was added to  $400 \mu\text{M}$  DNA solution (base concentration) to reach a final  $[\text{Cu}^{2+}]/[\text{base}]$  ratio of 0.1. Then concentrated MG solution was added to DNA-Cu(II) to reach a final concentration of  $40 \mu\text{M}$ . After incubation for 15 min, concentrated ofloxacin solution was quantitatively titrated into DNA-Cu(II)-MG solution. CD spectra were recorded from 700 nm to 190 nm at  $25^\circ\text{C}$  using a quartz cuvette of 0.5 cm pathlength.

### UV Spectroscopy

UV melting curves were collected on a Cary Varian UV/vis spectrophotometer equipped with a Peltier temperature controller. The melting profiles were monitored at 260 nm in a cuvette of 1 mm pathlength from  $15^\circ\text{C}$  to  $95^\circ\text{C}$  with the heating rate of  $0.6^\circ\text{C}/\text{min}$ .

### Isothermal Titration Calorimetry (ITC)

ITC experiments were performed using a MicroCal VP-ITC (MicroCal, Northampton, MA) with the sample cell (1.45 mL) containing  $200 \mu\text{M}$  DNA or DNA-Cu(II) (base concentration) in 10 mM Tris-HCl buffer (pH 7.0). Typically, 27 serial injections of  $500 \mu\text{M}$  *S*- or *R*-ofloxacin in Tris-HCl buffer of 10  $\mu\text{L}$  volume each were titrated in the sample cell at an interval of 180 s under continuous stirring at 307 rpm. The isothermal titration curves were corrected for heat of dilution by injecting ofloxacin solution into the buffer. The binding constant  $K_A$ , the stoichiometry  $N$ , and the enthalpy change  $\Delta H^0$  were obtained by fitting the integrated heats of binding isotherm according to the one-site binding model using MicroCal Origin 7.0 software.

### Fluorescence Spectroscopy

Fluorescence measurements were carried out on a Varian Cary Eclipse spectrophotometer equipped with a Peltier temperature controller. Fluorescence emission spectra were recorded from 500 nm to 750 nm at an excitation wavelength of 480 nm for EB. The samples were analyzed using a quartz cell with 1 cm pathlength, and slit widths for excitation and emission were set as 5 and 10 nm, respectively.

For competitive binding assays, DNA-Cu(II)-EB was prepared as follows: concentrated  $\text{CuCl}_2$  solution was added to  $50 \mu\text{M}$  DNA (base concentration) solution to reach a final  $[\text{Cu}^{2+}]/[\text{base}]$  ratio of 0.1. Then concentrated EB solution was added to DNA-Cu(II) to reach a final concentration of  $10 \mu\text{M}$ . After incubation for 15 min, concentrated ofloxacin solution was quantitatively titrated into DNA-Cu(II)-EB solution.

### Dynamic Light Scattering (DLS)

The size distribution of DNA and DNA-Cu(II)-ofloxacin complex was measured by using Zetasizer Nano ZS-90 (Malvern Instrument, UK). All the samples were detected at  $25^\circ\text{C}$  with a fixed wavelength of 633 nm and scattering angle of  $173^\circ$ . At least 10 parallel measurements were obtained for each sample.

### Atom Force Microscopy (AFM)

The effects of ofloxacin on the morphology of DNA were studied by AFM in the absence and presence of  $\text{Cu}^{2+}$ . The samples were prepared as follows:  $100 \mu\text{L}$  DNA solution (base concentration of  $800 \mu\text{M}$ ) was mixed with  $\text{Cu}^{2+}$ , *S*- or *R*-ofloxacin in Tris-HCl buffer (pH 7.0) for 15 min, and then diluted to a DNA concentration of  $1 \text{ ng}/\mu\text{L}$  using 10 mM Tris-HCl buffer containing 5 mM  $\text{MgCl}_2$ . A  $10\text{-}\mu\text{L}$  droplet of the diluted solution was dropped onto freshly cleaved mica ( $1 \times 1 \text{ cm}$ ). After adsorption for 5 min, the mica surface was rinsed with  $200 \mu\text{L}$  distilled water several times and dried in a gentle stream of nitrogen gas. All AFM images were recorded with Veeco Instruments Nanoscope IV in tapping mode. Silicon probes Tap300Al-G were used with a resonance frequency of 300 kHz. The scan frequency was 1 Hz per line. The height distributions were obtained through analyzing the height values of different sites ( $>100$ ) of DNA strands by Nanoscope software. The size distributions of distorted structures were obtained through analyzing the height values of different distortions ( $>100$ ) on DNA strands. The errors were represented by standard deviations.

### High-Performance Liquid Chromatography (HPLC)

The enantiomeric excess (*ee*) of ofloxacin enantiomers was analyzed by HPLC (Agilent 1200 Series), using a Kromasil  $\text{C}_{18}$  column ( $5 \mu\text{m}$ ,  $4.6 \times 250 \text{ mm}$ ) and a UV detector at 293 nm. The mobile phase contained a mixture of methanol/water (20/80, v/v), 2.5 mM L-isoleucine, and 0.6 mM  $\text{Cu}^{2+}$  at a flow rate of  $0.5 \text{ mL}/\text{min}$ .<sup>17</sup> The typical HPLC graphs and the standard curves of *S*- and *R*-ofloxacin are illustrated in Supporting Figures S1 and S2, respectively.

### Enantioseparation of Chiral Ofloxacin

Concentrated racemic ofloxacin aqueous solution (1 mM) was added to the as-prepared DNA solution ( $800 \mu\text{M}$ ,  $500 \mu\text{L}$ ) in the absence or presence of  $\text{Cu}^{2+}$  ( $[\text{Cu}^{2+}]/[\text{base}] = 0, 0.01, 0.1, 0.5$ ), to a final concentration of  $50 \mu\text{M}$ . After a 15-min incubation, the mixture was transferred to the spin column. After centrifugation at 8000 rpm for 20 min, the mixture was separated using the spin column. The concentration of *S*- and *R*-ofloxacin in the permeate solution was measured by HPLC, and the enantiomeric excesses are denoted *ee*,<sub>*P*</sub>, calculated by equation (1):

$$ee.P(\%) = \frac{(A_{R,P} - A_{S,P})}{(A_{R,P} + A_{S,P})} \times 100(\%) \quad (1)$$

where  $A_{R,P}$  and  $A_{S,P}$  are the peak areas of *R*- and *S*-enantiomer, respectively.

### Adsorption Isotherms of Ofloxacin Enantiomers

First, 10 mM  $\text{CuCl}_2$  was added quantitatively to the DNA solution ( $800 \mu\text{M}$ ,  $500 \mu\text{L}$ ) to reach the  $[\text{Cu}^{2+}]/[\text{base}]$  ratio of 0.01 and 0.1, respectively. After incubation for 15 min, concentrated *S*/*R*-ofloxacin aqueous solution was added to the obtained DNA-Cu(II) solution, to a final concentration of 25–300  $\mu\text{M}$ . After a 15-min incubation, the mixture was transferred to the spin column. After centrifugation at 8000 rpm for 20 min, the mixture solution was separated using the spin column. The concentration of *S*- and *R*-ofloxacin in the permeate solution was measured by HPLC. The resulting data were fitted to a Langmuir-Freundlich model represented as equation (2):

$$q = \frac{Q_{\max} (K_{\text{LF}} C_e)^n}{1 + (K_{\text{LF}} C_e)^n} \quad (2)$$

where  $q$  is the adsorbed amount of ofloxacin ( $\mu\text{mol}/\text{mg}$ ),  $C_e$  is the equilibrium concentration of ofloxacin enantiomer in the permeate ( $\mu\text{M}$ ),  $Q_{\max}$  is the adsorption capacity ( $\mu\text{mol}/\text{mg}$ ),  $K_{\text{LF}}$  is the Langmuir-Freundlich

constant (mL/mg), and  $n$  is the cooperativity coefficient. Generally, if  $n > 1$ , cooperativity was defined as positive, and if  $n < 1$ , cooperativity was negative.

The Scatchard test was carried out to evaluate the cooperative effects in the adsorption of ofloxacin enantiomers on the DNA or DNA-Cu(II), which is represented as equation (3):

$$\frac{q}{C_e} = \frac{q_{\max}}{K_d} - \frac{q}{K_d} \quad (3)$$

where  $q$  is the adsorbed amount of ofloxacin ( $\mu\text{mol/mg}$ ),  $C_e$  is the equilibrium concentration of ofloxacin in the permeate ( $\mu\text{M}$ ),  $q_{\max}$  is the adsorption capacity ( $\mu\text{mol/mg}$ ), and  $K_d$  is the dissociation constant (mL/mg). The shapes of the plots of  $q/C_e$  as a function of  $q$  were particularly sensitive to whether there were independent, dependent nonidentical, or cooperative interactions. If the shape of the plots was linear, an independent interaction between biomacromolecule and ligand existed. If it was convex, negative cooperativity was indicated. If it was asymptotic (or in some cases concave), positive cooperativity was observed.

## RESULTS AND DISCUSSION

### Structural Transition of Natural Polynucleotides Induced by Ofloxacin and $\text{Cu}^{2+}$

The effects of  $\text{Cu}^{2+}$  and ofloxacin on the structures of natural polynucleotides were studied using *Micrococcus lysodeikticus* DNA and calf thymus DNA, respectively. The base concentration of polynucleotides used in the enantioseparation is  $800 \mu\text{M}$  and the concentration range of  $\text{Cu}^{2+}$  is  $8\text{--}4000 \mu\text{M}$  (denoted as the molar ratios of  $[\text{Cu}^{2+}]/[\text{base}]$  in the range of  $0.01\text{--}5$ ). As shown in Figure 2a, the CD spectrum of ML DNA exhibits a positive band at  $272 \text{ nm}$  accompanied by a shoulder peak at  $285 \text{ nm}$  as well as a negative band around  $243 \text{ nm}$ . Upon titration with  $\text{Cu}^{2+}$ , the

intensity of the CD band at  $272 \text{ nm}$  gradually decreases until the  $[\text{Cu}^{2+}]/[\text{base}]$  ratio increases to 5. The plots of CD intensity at  $272 \text{ nm}$  show an obvious inflexion at the  $[\text{Cu}^{2+}]/[\text{base}]$  ratio of 0.75 (see the inset of Fig. 2a), indicating the conformational transition induced by  $\text{Cu}^{2+}$ . For CT DNA (Fig. 2b), the CD spectrum exhibits a positive peak at  $275 \text{ nm}$  and a negative band at  $245 \text{ nm}$ . With the  $[\text{Cu}^{2+}]/[\text{base}]$  ratio ranges from 0 to 2.0, the CD band at  $275 \text{ nm}$  gradually decreases, showing two inflexions at 0.3 and 2.0, respectively (see the inset of Fig. 2b). The melting temperature ( $T_m$ ) of CT DNA alone is  $70.2^\circ\text{C}$  in the absence of cationic ions. Upon addition of  $\text{Cu}^{2+}$  at the  $[\text{Cu}^{2+}]/[\text{base}]$  ratio of 0.01, 0.1, and 0.5, the  $T_m$  values were determined as  $71.0$ ,  $74.8$ , and  $73.5^\circ\text{C}$ , respectively, suggesting that the addition of  $\text{Cu}^{2+}$  ions enhance the thermal stability of CT DNA (Fig. 2c). The melting curve of ML DNA does not show a sigmoid shape, and it is impossible to obtain the effect of  $\text{Cu}^{2+}$  on the  $T_m$  of ML DNA.

In order to test the chiral discrimination of natural DNA regulated by  $\text{Cu}^{2+}$ , the enantiomeric excesses ( $e.e._p$ ) in the permeate were analyzed for racemic ofloxacin solution after being adsorbed by DNA and DNA-Cu(II) (shown in Fig. 2d). With increasing the  $[\text{Cu}^{2+}]/[\text{base}]$  ratio from 0.01 to 0.1, the  $e.e._p$  can be increased up to 65.6% (*R*-enantiomer excess) for ML DNA. Under the same  $[\text{Cu}^{2+}]/[\text{base}]$  ratio the highest  $e.e._p$  value reaches 55.6% in the case of CT DNA. And the  $e.e._p$  decreases as the  $[\text{Cu}^{2+}]/[\text{base}]$  ratio increases to 0.5. As a control, in the absence of  $\text{Cu}^{2+}$ , the  $e.e._p$  only increases to 15.1% for ML DNA and 10.4% CT DNA. Combining with CD spectra, UV melting profiles, as well as the enantioseparation results, either ML DNA or CT DNA exhibits enantioselective interaction toward *S*-ofloxacin at the

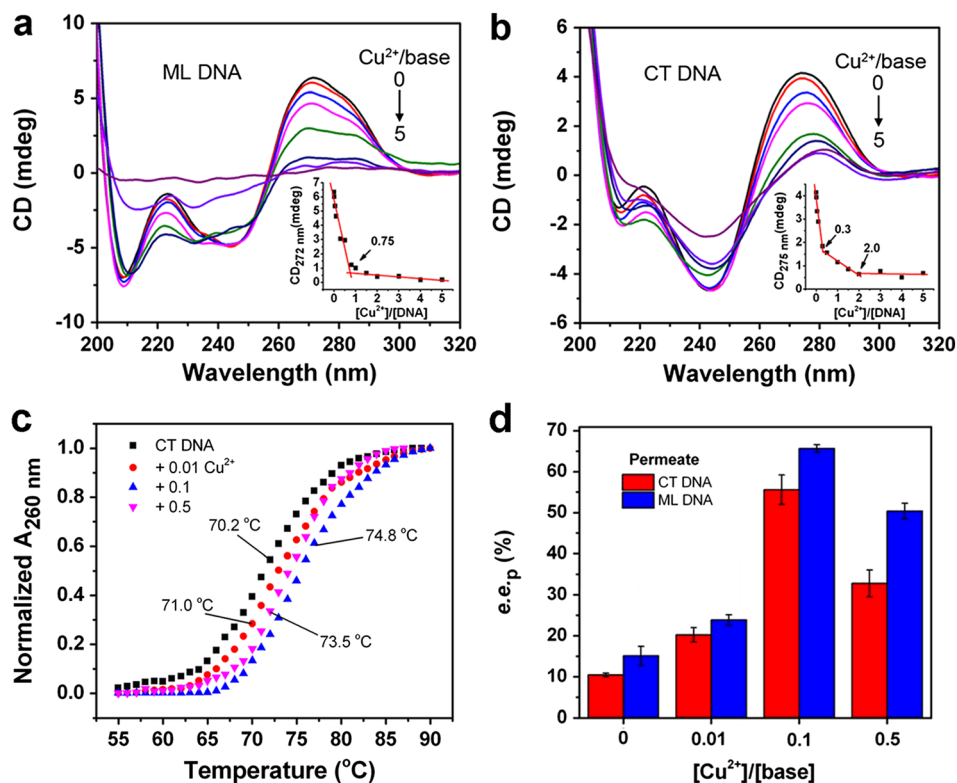


**Fig. 2.** CD spectra of  $800 \mu\text{M}$  (base concentration) ML DNA (a) and CT DNA (b) titrated with  $\text{Cu}^{2+}$  at pH 7.0. Inset: the intensities of CD bands at  $272 \text{ nm}$  for ML DNA and  $275 \text{ nm}$  for CT DNA versus the molar ratios of  $[\text{Cu}^{2+}]/[\text{base}]$ . (c) Normalized UV melting curves of CT DNA in the absence and presence of  $\text{Cu}^{2+}$  ( $[\text{Cu}^{2+}]/[\text{base}] = 0.01, 0.1, \text{ and } 0.5$ ) at pH 7.0, respectively. (d) The  $e.e._p$  values (*R*-excess) in the permeate solution of  $50 \mu\text{M}$  racemic ofloxacin after being adsorbed by  $800 \mu\text{M}$  DNA-Cu(II) complexes with different  $[\text{Cu}^{2+}]/[\text{base}]$  ratios at pH 7.0.

$[\text{Cu}^{2+}]/[\text{base}]$  ratio of 0.01~0.5, owing to the intrinsic chirality of natural polynucleotides modulated by  $\text{Cu}^{2+}$ .

Further, AFM images were measured to discern the morphological variations of natural DNA upon addition of ofloxacin enantiomer and/or  $\text{Cu}^{2+}$  ions. ML DNA alone displays a relaxed, thread-like structure with an average height of 0.45 nm, which is consistent with the height of a single uncondensed double-stranded DNA on the mica surface in a previous report (Fig. 3a).<sup>18</sup> At the  $[\text{Cu}^{2+}]/[\text{base}]$  ratio of 0.1, the average height of ML DNA-Cu(II) is determined as 0.46 nm, with no compaction discerned (Fig. 3b). Interestingly, *S*-ofloxacin induces a local folding transition of ML DNA in the presence of  $\text{Cu}^{2+}$  ( $[\text{Cu}^{2+}]/[\text{base}]=0.1$ ). With the addition

of 25  $\mu\text{M}$  *S*-ofloxacin, structural distortions appear along the thread-like DNA, and the average height of these distorted structures was measured as 0.82 nm (Fig. 3c). As the concentration of *S*-ofloxacin increases to 100  $\mu\text{M}$ , these distortions become larger, with an average height of 1.38 nm (Fig. 3d). Meanwhile, some short rods can be observed along the DNA strands under these conditions. The distortions on these DNA strands might be attributed to DNA bending caused by the binding of *S*-ofloxacin. Apparently, the folding transition of ML DNA induced by *S*-ofloxacin is a segregated state, where the same DNA molecule is composed of distorted structures and unfolded parts (Fig. 3e). In contrast, upon addition of 100  $\mu\text{M}$  *R*-ofloxacin, the average size of the

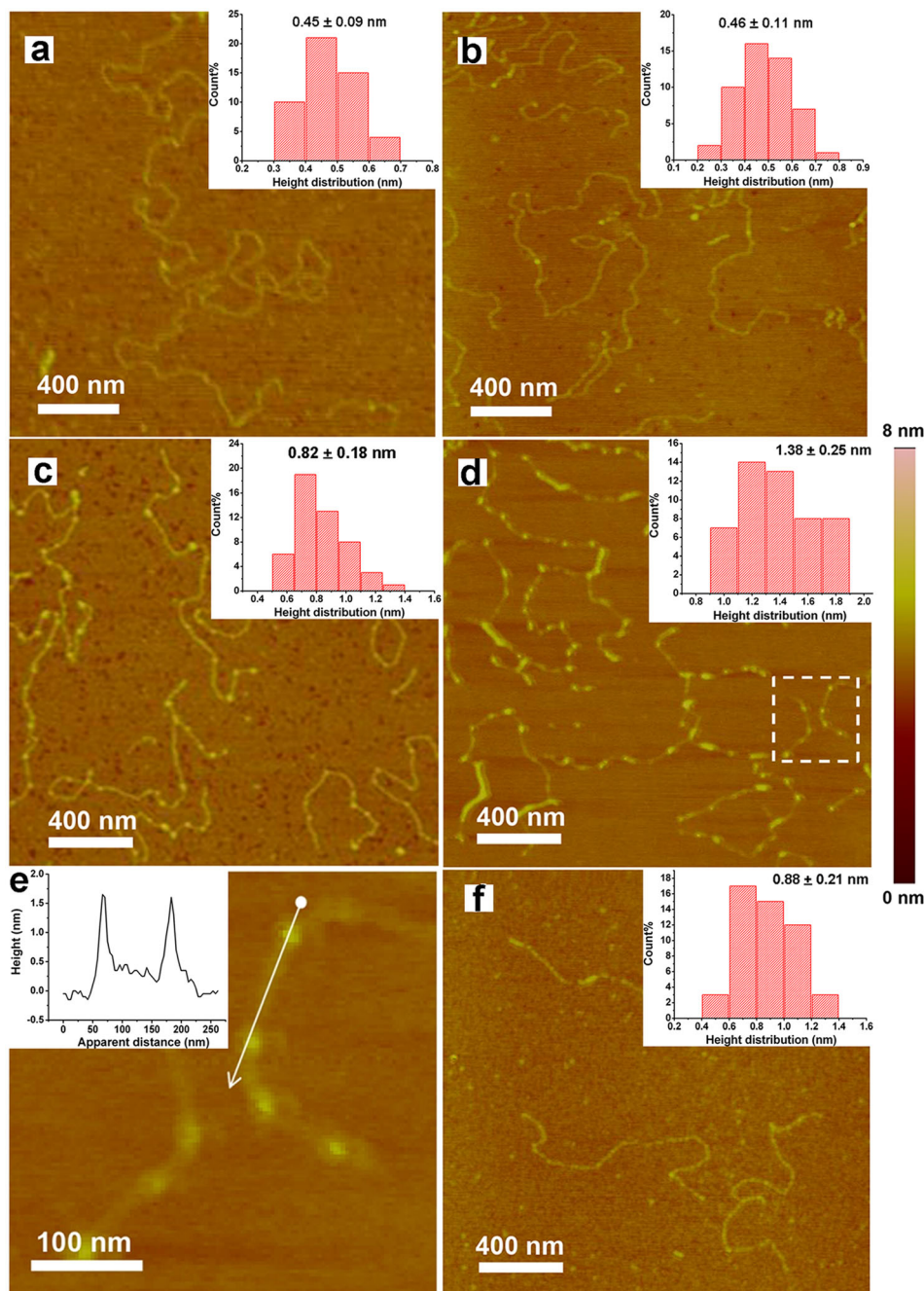


**Fig. 3.** AFM images of ML DNA alone (a) and DNA-Cu(II) at the  $[\text{Cu}^{2+}]/[\text{base}]$  ratio of 0.1 (b), the insets of (a,b) are the height distributions of DNA strands. DNA-Cu(II) ( $[\text{Cu}^{2+}]/[\text{base}]=0.1$ ) incubated with 25  $\mu\text{M}$  *S*-ofloxacin (c), 100  $\mu\text{M}$  (d) *S*-ofloxacin, as well as 100  $\mu\text{M}$  *R*-ofloxacin (f), the insets of (c,d,f) are the size distributions of distortions on DNA strands. The size of (a,b,c,d,f) is  $2 \times 2 \mu\text{m}$ , and (e) is a zoomed image of the squared area in (d).

induced distortions only reaches 0.88 nm (Fig. 3f). Similar structural distortions can also be detected for CT DNA in the presence of  $\text{Cu}^{2+}$  and *S*-ofloxacin (Fig. S3a,b). Therefore, *S*-ofloxacin is more liable to induce the locally distorted structures of polynucleotides in the presence of  $\text{Cu}^{2+}$ , compared to its *R*-enantiomer. According to DLS measurements (Table 1), the hydrodynamic diameter ( $d_1$ ) of ML DNA decreases from 1975 to 851 nm, while the  $d_2$  value increases from 103 to 120 nm upon addition of *S*-ofloxacin and  $\text{Cu}^{2+}$ . A similar trend is found for CT DNA under the same conditions. In the absence of  $\text{Cu}^{2+}$ , after incubation with *S*-ofloxacin, no apparent distortion is observed in the AFM image (Fig. S3c). Moreover, slight changes in the size distributions are detected according to the DLS results. It is demonstrated that ofloxacin and  $\text{Cu}^{2+}$  have cooperative effects on the local distortions of natural polynucleotides.

Organometallic compounds including Pt(II) and Ru(II) complexes as well as transition metal ions have been reported to bend the DNA helix toward its major groove, resulting in the characteristic DNA distortions.<sup>19–21</sup> For example, cisplatin bound at N7 sites of purines to form di-adducts with DNA, and micro-loops appeared through distant crosslinks due to the induced local distortions. Then the whole DNA molecule was condensed into a compact globule through further crosslinks. Combined with our previous studies, it is reasonable to conclude that the distance between adjacent base pairs is liable to be enlarged upon  $\text{Cu}^{2+}$ -assisted partial intercalation of ofloxacin in the minor groove, potentially bending the DNA helix toward the major groove. These locally distorted structures are recognized as an important feature of the effects of ofloxacin on the folding transition of polynucleotides in the presence of  $\text{Cu}^{2+}$ . All of the genome DNA in living cells is above the size of several hundred thousand base pairs, which can undergo a dramatic conformational transition from a wormlike coil to a much smaller globular state in the presence of multivalent cations, proteins, cationic lipids, and positively charged nano-objects.<sup>22</sup> This phenomenon, known as DNA compaction, is a key biological process involved in the packaging of genetic information as well as in gene regulation since the compact region is inaccessible to DNA transaction machinery. Although several reports have presented the effects of enantiomeric dications on DNA compaction,<sup>6,7</sup> the effects of chiral drugs on the folding transition of DNA have not been thoroughly investigated. Further characterizations of the interactions between ofloxacin and DNA are needed to disclose the mechanism of the observed local distortions.

**TABLE 1.** The hydrodynamic diameter of ML and CT DNA in the absence and presence of  $\text{Cu}^{2+}$  and ofloxacin

Specimen	$d_1$ (nm)	$d_2$ (nm)	$d_3$ (nm)
ML DNA <sup>a</sup>	1974.8±93.9	103.1±15.8	—
ML DNA- <i>S</i> -enantiomer <sup>b</sup>	1857.3±27.8	94.2±4.5	—
ML DNA-Cu(II)- <i>S</i> -enantiomer <sup>c</sup>	851.4±23.3	119.8±15.0	34.0±12.8
CT DNA <sup>a</sup>	1579.5±90.6	105.2±7.7	—
CT DNA- <i>S</i> -enantiomer <sup>b</sup>	1530.3±91.4	112.8±11.1	—
CT DNA-Cu(II)- <i>S</i> -enantiomer <sup>c</sup>	789.2±53.8	108.1±7.9	24.9±3.3

<sup>a</sup>The base concentration of DNA is 60  $\mu\text{M}$ .

<sup>b</sup>The concentration of *S*-ofloxacin is 100  $\mu\text{M}$ .

<sup>c</sup>The molar ratio of  $[\text{Cu}^{2+}]/[\text{base}]$  is 0.1.

Chirality DOI 10.1002/chir

### Enantioselective Recognition of Chiral Ofloxacin by Polynucleotides

In order to reveal the mechanism of ofloxacin-induced DNA distortion, interactions between DNA and ofloxacin were investigated by using ITC measurements and competitive binding assays. ITC profiles for two enantiomers binding to ML DNA were performed at the  $[\text{Cu}^{2+}]/[\text{base}]$  ratio of 0.1 (shown in Fig. 4). The stronger exothermicity was detected in the complexation of DNA-Cu(II) with *S*-ofloxacin compared with the *R*-enantiomer, suggesting that DNA-Cu(II) preferentially binds to the *S*-enantiomer. The association constant ( $K_A$ ) of DNA-Cu(II) and *S*-ofloxacin was determined as  $1.89 \times 10^5 \text{ M}^{-1}$ , which is three times higher than that of the *R*-enantiomer. However, in the absence of  $\text{Cu}^{2+}$ , less exothermicity occurs in the binding of *S*-ofloxacin to DNA, and it is difficult to find a suitable binding model for this profile (Fig. S4a). The thermodynamic parameters  $\Delta_b H$  and  $\Delta_b S$  obtained from the best fitting clearly

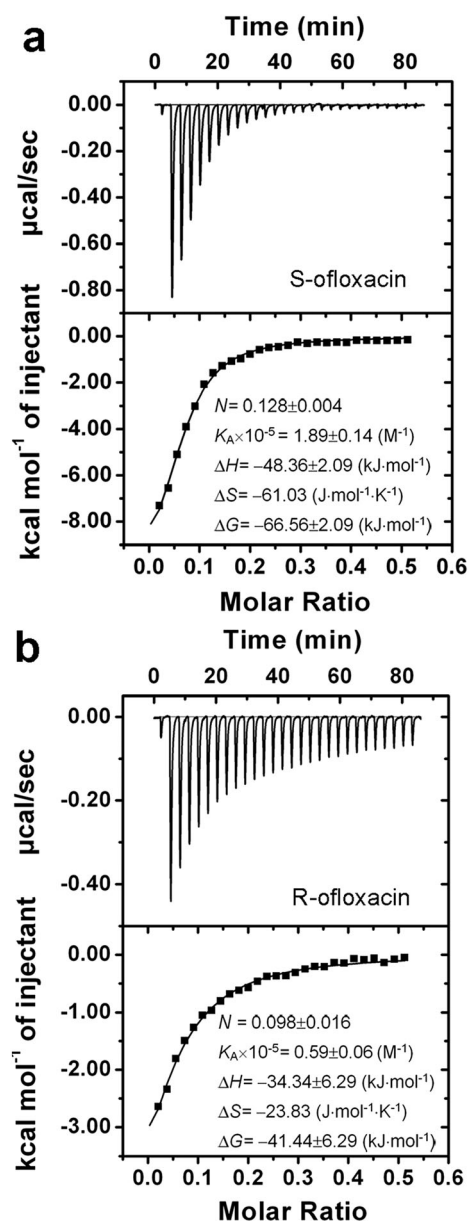


**Fig. 4.** ITC profiles for the titrations of (a) *S*- and (b) *R*-ofloxacin into ML DNA-Cu(II) ( $[\text{Cu}^{2+}]/[\text{base}]=0.1$ ) at pH 7.0.

indicate that this binding is a strong enthalpy-driven process accompanied by an unfavorable entropy contribution. For intercalator ethidium and daunorubicin, their binding processes were driven by enthalpy with opposing enthalpic and entropic contributions, and their unfavorable entropy correlated with the extent of DNA distortion due to the intercalation. In contrast, for the groove binder Hoechst 33258, its binding process was entropically driven, with an unfavorable positive enthalpy. There was little perturbation of the DNA secondary structure with the ligand fitting into its minor groove. According to the thermodynamic parameters involved in the binding process of ofloxacin onto ML DNA-Cu(II), it is indicated that the unfavorable entropy mainly results from the conformational transition from the elongated coil to the local distorted state induced by partial intercalation.<sup>23,24</sup> In the case of CT DNA-Cu(II) ( $[Cu^{2+}]/[base]=0.1$ ), the  $K_A$  value was determined as  $2.79 \times 10^5 M^{-1}$  for *S*-ofloxacin, whereas the binding for *R*-ofloxacin is too weak to be detected (Fig. S4b,c).

In order to investigate the binding site of ofloxacin to DNA-Cu(II), the competitive binding assays were carried out by using methyl green (MG) and ethidium bromide (EB) as the probes.<sup>25</sup> It is well known that EB can intercalate into the DNA double helix from the minor groove, which results in a great enhancement of its fluorescence emission at 480 nm. Adopting ML DNA, titrations of *S*-ofloxacin into the as-prepared DNA-Cu(II)-EB result in a significant decrease of fluorescence emission at 480 nm (Fig. 5a), which suggests that *S*-ofloxacin excludes the bound EB molecules from DNA-Cu(II). As MG binds to the major groove of DNA, a

series of CD bands at 310 nm, 430 nm, 620 nm, and 650 nm can be induced, as shown in Figure 5b. With titrating *S*-ofloxacin into the obtained DNA-Cu(II)-MG, all the induced CD bands are maintained even at high concentrations of drug, indicating that MG molecules cannot dissociate from DNA. Moreover, a fairly similar trend is obtained for CT DNA (Fig. S5). Combined with the ITC results, it is reasonable to conclude that ofloxacin partially intercalates into the DNA double-helix from its minor groove.

The interaction mechanism is further approved through the response of DNA-Cu(II)-ofloxacin complex toward external stimulus. Upon addition of EDTA into the DNA-Cu(II)-ofloxacin at pH 7.0, the CD band shifts from 285 nm to 272 nm, which suggests that the strong chelation of  $Cu^{2+}$  by EDTA induces the release of ofloxacin molecules from DNA. By adding equimolar EDTA and  $Cu^{2+}$  alternately, the CD spectra can be tuned reversibly (Fig. 5c). Moreover, the CD band shifts reversibly from 285 nm to 272 nm owing to the pH level changing between 7.0 and 9.0, which results from the pH-responsive interaction between ofloxacin and DNA in the presence of  $Cu^{2+}$  (Fig. 5d). The spectral reversibility triggered by  $Cu^{2+}$  and pH suggests that the assembly of DNA-Cu(II)-ofloxacin is most probably controlled by the reversible coordination and the electrostatic interactions. Although it is hard to determine the exact sequence composition of natural polynucleotides, it can be deduced that ofloxacin interacts with DNA through coordination, electrostatic, as well as other weak strengths such as hydrophobic forces and/or  $\pi$ - $\pi$  stacking.

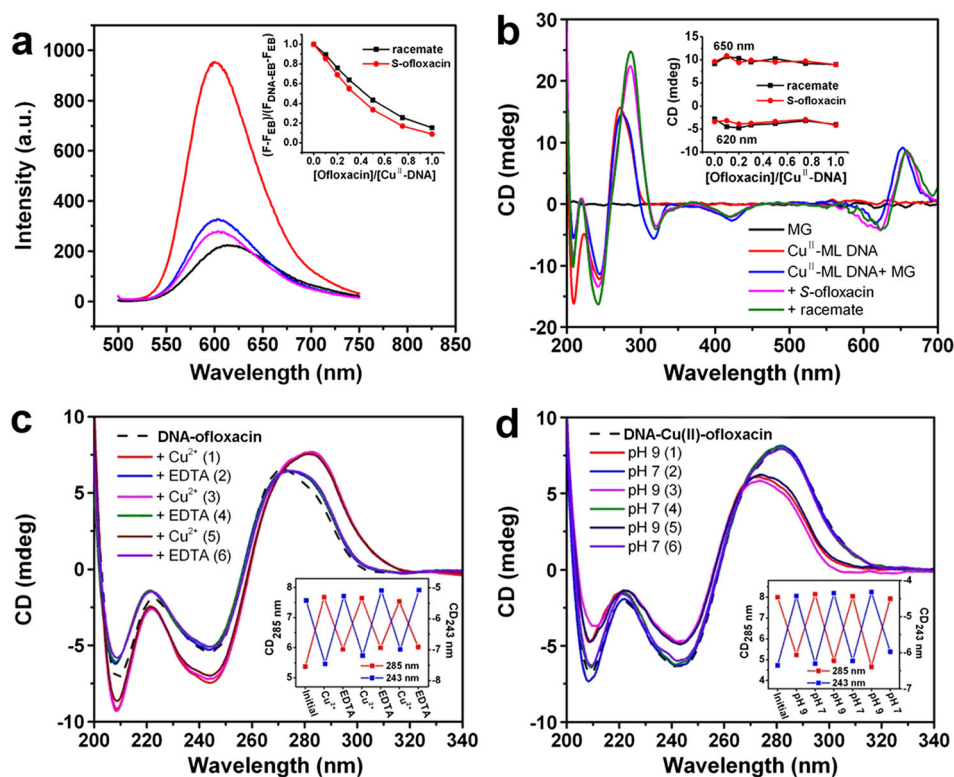


**Fig. 5.** (a) Fluorescence emission spectra of EB (black), ML DNA-Cu(II)-EB (red), and ML DNA-Cu(II)-EB upon addition of *S*- (pink) or racemic ofloxacin (blue). Inset: Plots of relative fluorescence changes at 480 nm with the molar ratios  $[ofloxacin]/[base]$ ; The concentrations of DNA and EB are  $50 \mu M$  and  $10 \mu M$ , respectively,  $[Cu^{2+}]/[base]=0.1$ . (b) CD spectra of MG, ML DNA-Cu(II), ML DNA-Cu(II)-MG upon addition of *S*- or racemic ofloxacin. Inset: Plots of the changes of CD bands at 650 nm and 620 nm with the molar ratios  $[ofloxacin]/[base]$ . The concentration of DNA and MG are  $400 \mu M$  and  $40 \mu M$ , respectively,  $[Cu^{2+}]/[base]=0.1$ . CD spectra of ML DNA-Cu(II)-ofloxacin ( $[Cu^{2+}]/[base]=0.1$ ,  $50 \mu M$  racemic ofloxacin) treated by (c) alternately adding equivalent moles of EDTA and  $Cu^{2+}$ , and (d) reversibly adjusting the pH value between 7.0 and 9.0. Inset: the reversible changes of CD intensities at 285 nm and 243 nm, respectively.

### Adsorption Mechanism of Ofloxacin Enantiomers on Polynucleotides Regulated by $\text{Cu}^{2+}$

The adsorption isotherms of ofloxacin enantiomers onto DNA and DNA-Cu(II) are depicted in Figure 6a,b, respectively. Among Langmuir, Freundlich, and Langmuir–Freundlich (LF) models, it is indicated that the LF model fits the data well at the  $[\text{Cu}^{2+}]/[\text{base}]$  ratio of 0–0.1. Maximum adsorption capacities ( $Q_{\text{max}}$ ), Langmuir–Freundlich constants ( $K_{\text{LF}}$ ), and the cooperativity coefficient ( $n$ ) of *S*- and *R*-ofloxacin are listed in Table 2. Adopting ML DNA, the  $Q_{\text{max}}$  values of *S*- and *R*-enantiomers are calculated as 0.20 and 0.17  $\mu\text{mol}/\text{mg}$ , respectively. At the  $[\text{Cu}^{2+}]/[\text{base}]$  ratio of 0.01, the  $Q_{\text{max}}$  of *S*-ofloxacin slightly increases to 0.22  $\mu\text{mol}/\text{mg}$ , while the  $Q_{\text{max}}$  of *R*-ofloxacin remains 0.17  $\mu\text{mol}/\text{mg}$ . Both enantioselectivity

and binding affinity of DNA toward *S*-ofloxacin are slightly enhanced compared with DNA alone. As increasing the  $[\text{Cu}^{2+}]/[\text{base}]$  ratio to 0.1, the  $Q_{\text{max}}$  values reach to 0.34 and 0.28  $\mu\text{mol}/\text{mg}$  for *S*- and *R*-ofloxacin, respectively. Compared with DNA alone, the  $K_{\text{LF}}$  values of both *S*- and *R*-ofloxacin are increased by more than three times at the  $[\text{Cu}^{2+}]/[\text{base}]$  ratio of 0.1. Therefore, it is demonstrated that Cu(II)-coordination enhances the binding affinities of ofloxacin to DNA. In this study, all the  $n$  values are higher than 1, which reveals that positive cooperativity exists in the adsorption of ofloxacin on DNA.<sup>26,27</sup> A fairly similar trend is obtained using CT DNA as the selector, however, the values of  $Q_{\text{max}}$  and  $K_{\text{LF}}$  of *S*- and *R*-ofloxacin, respectively, are lower than those of ML DNA (Table 2, Figs. S6, S7).

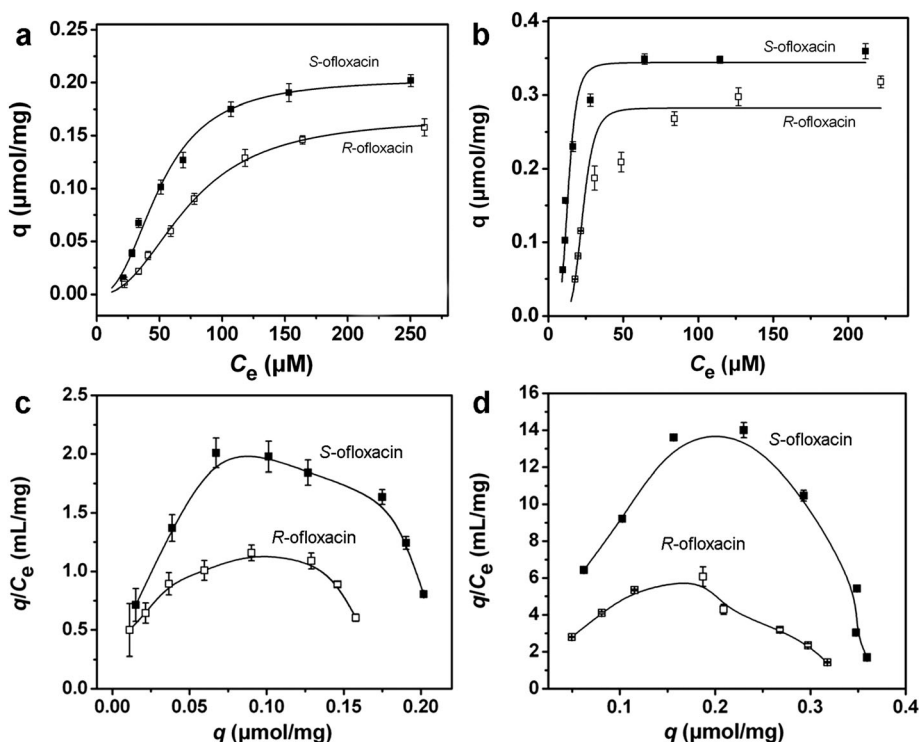


**Fig. 6.** Adsorption isotherms of ofloxacin on (a) ML DNA and (b) ML DNA-Cu(II) ( $[\text{Cu}^{2+}]/[\text{base}]=0.1$ ) at 25°C; Scatchard analysis of the adsorption of ofloxacin on (c) ML DNA and (d) ML DNA-Cu(II) ( $[\text{Cu}^{2+}]/[\text{base}]=0.1$ ) at 25°C.

**TABLE 2.** Calculated adsorption parameters of *S*- and *R*-ofloxacin on DNA and DNA-Cu(II) according to Langmuir-Freundlich model

Adsorbent	Enantiomer	$Q_{\text{max}}$ ( $\mu\text{mol}/\text{mg}$ )	$K_{\text{LF}}$ ( $\text{mL}/\text{mg}$ )	$n$	$R^2$
ML DNA	S	0.20	19.8	2.4	0.98
	R	0.17	13.6	2.4	0.99
ML DNA-Cu(II) (0.01 <sup>a</sup> )	S	0.22	22.6	2.6	0.99
	R	0.17	13.1	1.9	0.99
ML DNA-Cu(II) (0.1 <sup>a</sup> )	S	0.34	75.3	4.8	0.97
	R	0.28	43.5	6.0	0.96
CT DNA	S	0.11	15.9	3.7	0.99
	R	0.08	11.9	2.6	0.99
CT DNA-Cu(II) (0.01 <sup>a</sup> )	S	0.11	19.7	1.6	0.98
	R	0.09	8.9	1.3	0.99
CT DNA-Cu(II) (0.1 <sup>a</sup> )	S	0.29	84.7	8.3	0.95
	R	0.21	46.4	8.6	0.95

<sup>a</sup>The molar ratio of  $[\text{Cu}^{2+}]/[\text{base}]$ .

The test of Scatchard, the plot of  $q/C_e$  as a function of  $q$ , was performed to evaluate the presence of cooperative effects in drug adsorption (Fig. 6c,d). The nonlinearities of all the Scatchard plots suggest the presence of cooperative effects during ofloxacin adsorption.<sup>28</sup> It can be concluded that adsorption energies are lowered through the conformational transition of DNA induced by ofloxacin binding (the local distortions as shown in Fig. 3). Moreover, the maxima of the curvilinear Scatchard plot is determined as 0.075  $\mu\text{mol}/\text{mg}$  for ML DNA, and this  $q$  value shifts to 0.20  $\mu\text{mol}/\text{mg}$  at the  $[\text{Cu}^{2+}]/[\text{base}]$  ratio of 0.1. This suggests an increase of binding cooperativity and a change of adsorption mechanism upon Cu(II)-coordination. This change is an indication of Cu(II)-induced variations in the relative contribution of electrostatic, coordination interactions as well as other weak strengths such as hydrophobic and/or stacking interactions in the adsorption of ofloxacin on DNA. The studies on the adsorption behavior not only reveal the adsorption mechanism of ofloxacin enantiomers on natural polynucleotides, but provide fundamental data to develop novel enantioseparation methods.

### CONCLUSION

Natural polynucleotides including *Micrococcus lysodeikticus* DNA and calf thymus DNA were used to study the  $\text{Cu}^{2+}$ -regulated chiral discrimination of ofloxacin enantiomers. Both ML and CT DNA exhibit enantioselective recognition for *S*-ofloxacin in the presence of  $\text{Cu}^{2+}$ . Interestingly, ofloxacin and  $\text{Cu}^{2+}$  have cooperative effects on the local distortions of polynucleotides. In the presence of  $\text{Cu}^{2+}$ , *S*-ofloxacin is more liable to induce the locally distorted structures of polynucleotides compared to its *R*-enantiomer, and these observed structures are recognized as an important feature of the effects of ofloxacin on the folding transition of polynucleotides. The association constant of DNA-Cu(II) with *S*-ofloxacin is three times higher than that of *R*-enantiomer. This binding is a strong enthalpy-driven process accompanied by an unfavorable entropy contribution, which results from the conformational transition from the elongated coil to the locally distorted state induced by the partial intercalation of *S*-ofloxacin. The apparent increase of adsorption capability and cooperativity, as well as the change of adsorption mechanism, were detected in the adsorption of ofloxacin enantiomers on polynucleotides upon Cu(II)-coordination.

### SUPPORTING INFORMATION

Additional supporting information may be found in the online version of this article at the publisher's web-site.

### LITERATURE CITED

- Liu B, Han L, Che S. Formation of enantiomeric impeller-like helical architectures by DNA self-assembly and silica mineralization. *Angew Chem Int Ed* 2012; 51: 923–927.
- Roelfes G, Feringa BL. DNA-based asymmetric catalysis. *Angew Chem Int Ed* 2005; 44: 3230–3232.
- Zhang L, Song M, Tian Q, Min S. Chiral separation of l,d-tyrosine and l,d-tryptophan by ct DNA. *Sep Purif Technol* 2007; 55: 388–391.
- Li W, Li Y, Fu Y, Zhang J. Enantioseparation of chiral ofloxacin using biomacromolecules. *Korean J Chem Eng* 2013; 30: 1448–1453.
- Qu X, Trent JO, Fokt I, Priebe W, Chaires JB. Allosteric, chiral-selective drug binding to DNA. *Proc Natl Acad Sci U S A* 2000; 97: 12032–12037.
- Ito M, Sakakura A, Miyazawa N, Murata S, Yoshikawa K. Nonspecificity induces chiral specificity in the folding transition of giant DNA. *J Am Chem Soc* 2003; 125: 12714–12715.
- Zinchenko AA, Sergeev VG, Kabanov VA, Murata S, Yoshikawa K. Stereoisomeric discrimination in DNA compaction. *Angew Chem Int Ed* 2004; 43: 2378–2381.
- Zhang HY, Liu YR, Ji C, Li W, Dou SX, Xie P, Wang WC, Zhang LY, Wang PY. Oxaliplatin and its enantiomer induce different condensation dynamics of single DNA molecules. *PLoS One* 2013; 8:e71556.
- Matsuoka Y, Kanda N, Lee YM, Higuchi A. Chiral separation of phenylalanine in ultrafiltration through DNA-immobilized chitosan membranes. *J Mem Sci* 2006; 280: 116–123.
- Lee EJ, Yeo JA, Jung K, Hwangbo HJ, Lee GJ, Kim SK. Enantioselective binding of ofloxacin to B form DNA. *Arch Biochem Biophys* 2001; 395: 21–24.
- Hwangbo HJ, Yun BH, Cha JS, Kwon DY, Kima SK. Enantioselective binding of *S*- and *R*-ofloxacin to various synthetic polynucleotides. *Eur J Pharm Sci* 2003; 18: 197–203.
- Hayakawa I, Atarashi S, Yokohama S, Imamura M, Sakano K, Furukawa M. Synthesis and antibacterial activities of optically active ofloxacin. *Antimicrob Agents Chemother* 1986; 29: 163–164.
- Drew RH, Gallis HA. Ofloxacin: its pharmacology, pharmacokinetics, and potential for clinical application. *Pharmacotherapy* 1988; 8: 35–46.
- Fu Y, Duan X, Chen X, Zhang J, Li W. Enantioselective separation of chiral ofloxacin using functional Cu(II)-coordinated G-rich oligonucleotides. *RSC Adv* 2014; 4: 1329–1333.
- Fu Y, Duan X, Chen X, Zhang H, Zhang J, Li W. Chiral discrimination of ofloxacin enantiomers using DNA double helix regulated by metal ions. *Chirality* 2014; 26: 249–254.
- Li W, Chen X, Fu Y, Zhang J. Enantioselective recognition mechanism of ofloxacin via Cu(II)-modulated DNA. *J Phys Chem B* 2014; 118: 5300–5309.
- Tian ML, Row HS, Row KH. Chiral separation of ofloxacin enantiomers by ligand exchange chromatography. *Monatsh Chem* 2010; 141: 285–290.
- Hou XM, Zhang XH, Wei KJ, Ji C, Dou SX, Wang WC, Li M, Wang PY. Cisplatin induces loop structures and condensation of single DNA molecules. *Nucleic Acids Res* 2009; 37: 1400–1410.
- Gossens C, Tavernelli I, Rothlisberger U. DNA structural distortions induced by ruthenium-arene anticancer compounds. *J Am Chem Soc* 2008; 130: 10921–10928.
- Liu Z, Tan S, Zu Y, Fu Y, Meng R, Xing Z. The interactions of cisplatin and DNA studied by atomic force microscopy. *Micron* 2010; 41: 833–839.
- Rai P, Wemmer DE, Linn S. Preferential binding and structural distortion by  $\text{Fe}^{2+}$  at RGGG-containing DNA sequences correlates with enhanced oxidative cleavage at such sequences. *Nucleic Acids Res* 2005; 33: 497–510.
- Zhou T, Llizo A, Wang C, Xu G, Yang Y. DNA compaction: fundamentals and applications. *Soft Matter* 2011; 7: 6746–6756.
- Lin PH, Tong SJ, Louis SR, Chan Y, Chen WY. Thermodynamic basis of chiral recognition in a DNA aptamer. *Phys Chem Chem Phys* 2009; 11: 9744–9750.
- Bishop GR, Ren JS, Polander BC, Jeanfreau BD, Trent JO, Chaires JB. Energetic basis of molecular recognition in a DNA aptamer. *Biophys Chem* 2007; 126: 165–175.
- Zhao C, Ren J, Gregoliński J, Lisowski J, Qu X. Contrasting enantioselective DNA preference: chiral helical macrocyclic lanthanide complex binding to DNA. *Nucleic Acids Res* 2012; 40: 8186–8196.
- Rodríguez-Ruiz I, Delgado-Lopez JM, Duran-Olivencia MA, Iafisco M, Tampieri A, Colangelo D, Prat M, Gomez-Morales J. pH-responsive delivery of doxorubicin from citrate-apatite nanocrystals with tailored carbonate content. *Langmuir* 2013; 29: 8213–8221.
- Iafisco M, Di Foggia M, Bonora S, Prat M, Roveri N. Adsorption and spectroscopic characterization of lactoferrin on hydroxyapatite nanocrystals. *Dalton Trans* 2011; 40: 820–827.
- Sharma S, Agarwal GP. Interactions of proteins with immobilized metal ions — Role of ionic strength and pH. *J Colloid Interface Sci* 2001; 243: 61–72.